SUPPORTING INFORMATIONS:

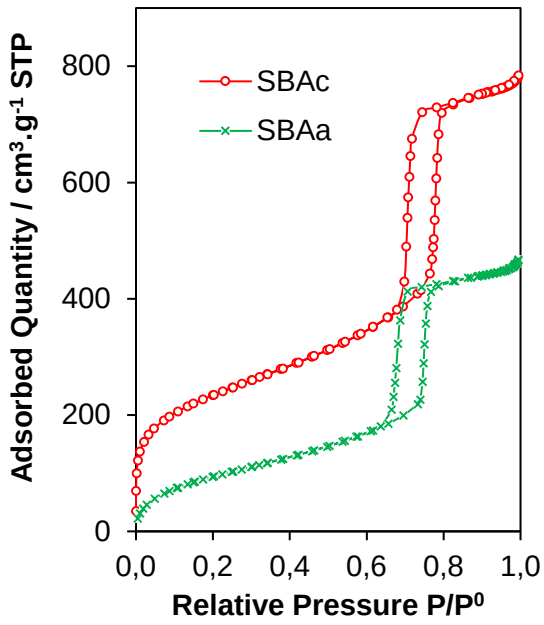

Figure S1: Adsorption / desorption isotherms of calcined (SBAc) and uncalcined (SBAa) SBA-15.

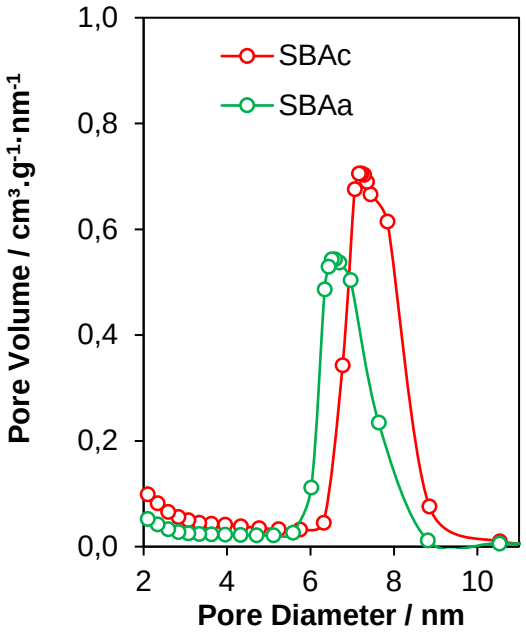

Figure S2: Pore size distribution of calcined (SBAc) and uncalcined (SBAa) SBA-15.

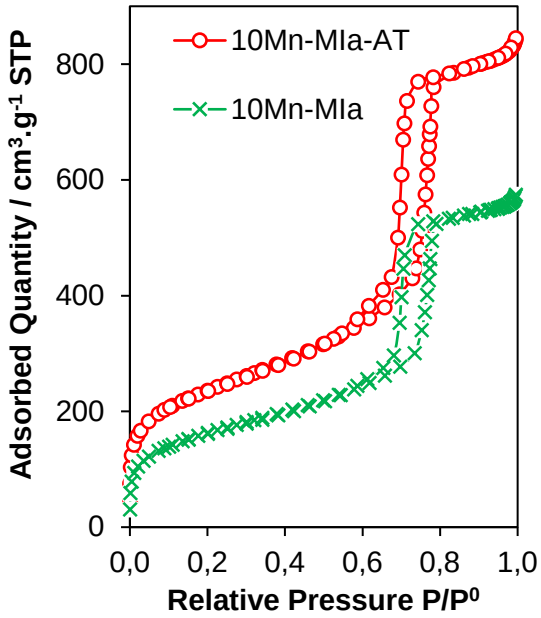

Figure S3: N_2 Adsorption/desorption isotherms of 10Mn-MIa before and after acid treatment

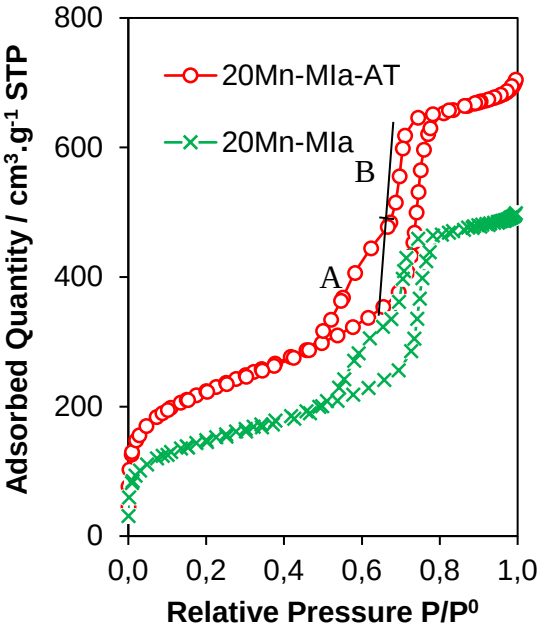

Figure S4: N_2 Adsorption/desorption isotherms of of 20Mn-MIa before and after acid treatment

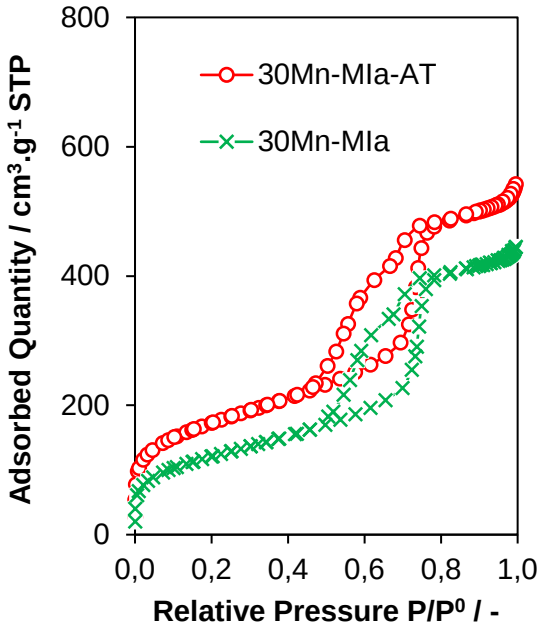

Figure S5: N_2 Adsorption/desorption isotherms of 30Mn-MIa before and after acid treatment

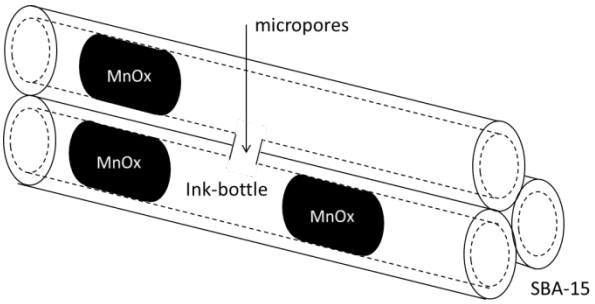

Figure S6: Scheme illustrating the "pore network effect" generating ink bottle pores[32]

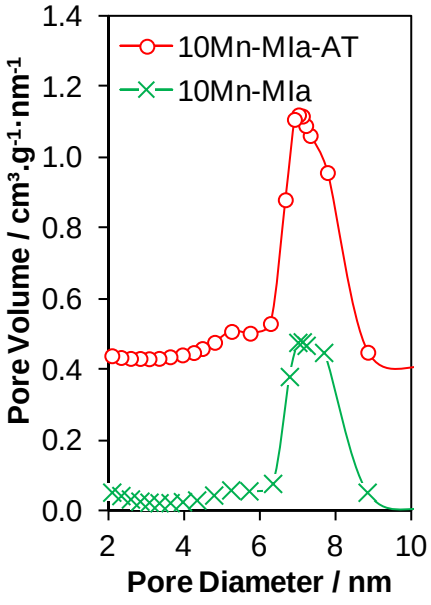

Figure S7: Pore size distribution (offset by 0.4 $cm^3.g^{-1}.nm^{-1}$) of 10Mn-MIa before and after acid treatment

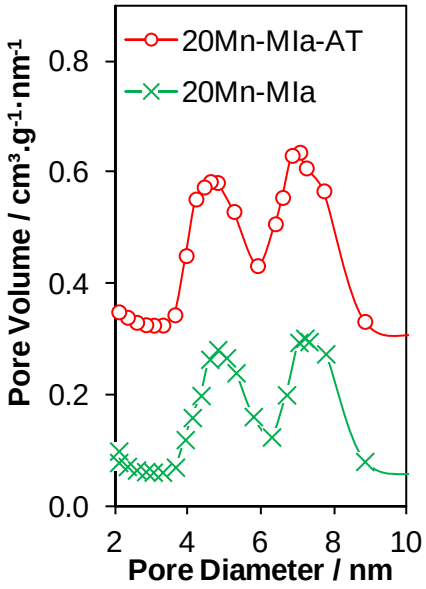

Figure S8: Pore size distribution (offset by 0.4 $cm^3.g^{-1}.nm^{-1}$) of 20Mn-MIa before and after acid treatment

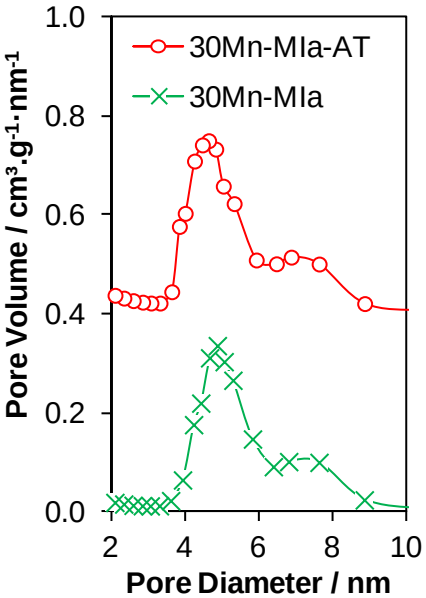

Figure S9: Pore size distribution (offset by 0.4 $cm^3.g^{-1}.nm^{-1}$) of 30Mn-MIa before and after acid treatment

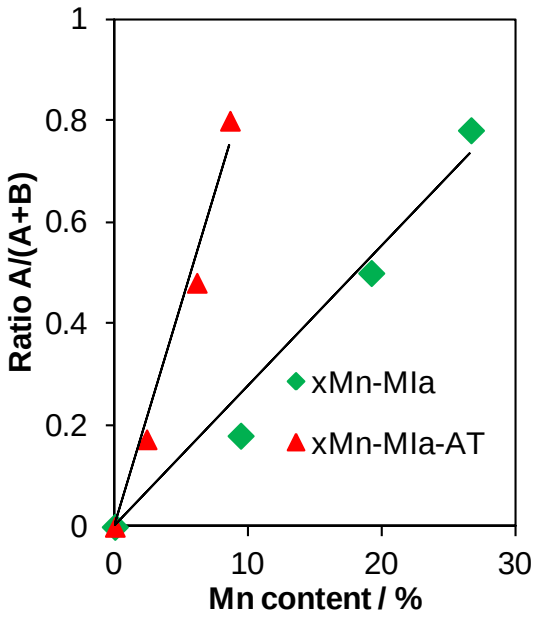

Figure S10: A/(A+B) ratio as a function of Mn wt %

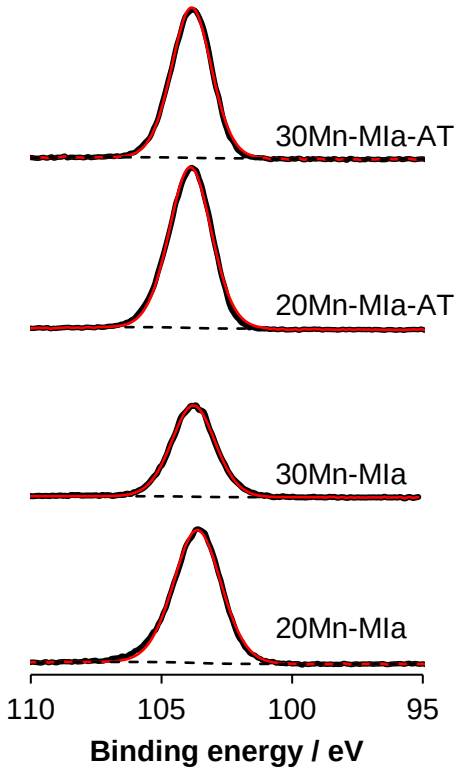

Figure S11: XPS spectra of Si 2p for 20 and 30 Mn-MIa before and after acid treatment

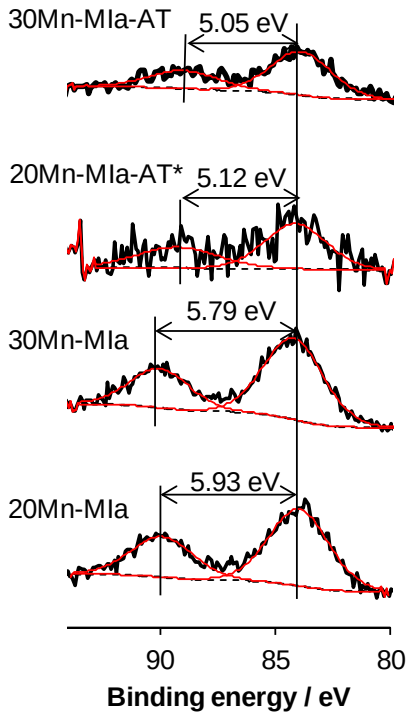

Figure S12: XPS spectra of Mn 3s for 20 and 30 Mn-MIa before and after acid treatment (* : gain x3)

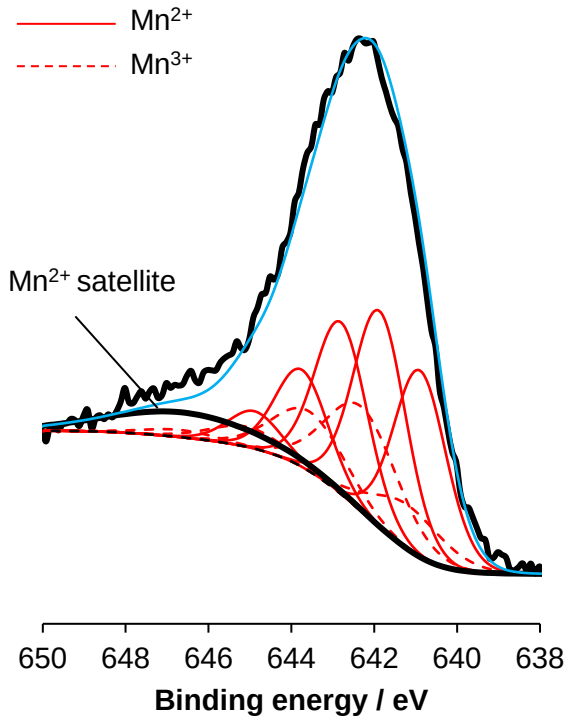

Figure S13: Example of the decomposition of Mn $2p_{3/2}$ envelope for 20Mn-MIa

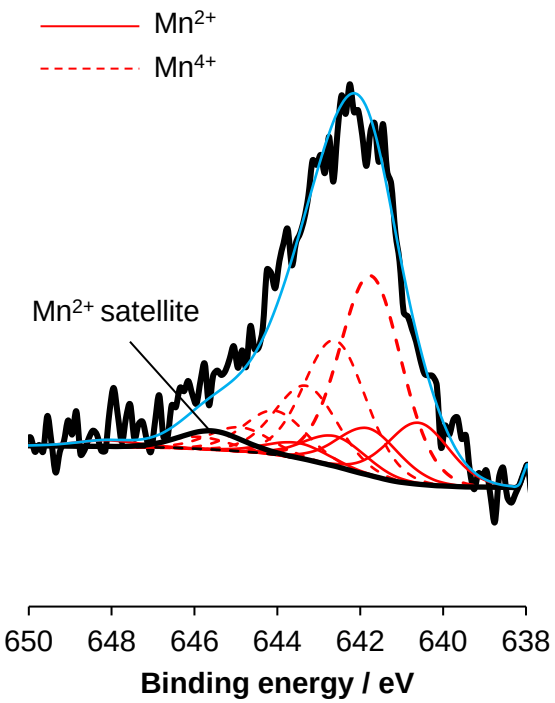

Figure S14: Example of the decomposition of Mn $2p_{3/2}$ envelope for 20Mn-MIa-AT

Table S1: Fitting parameters used to simulate the Mn $2p_{3/2}$ envelope for xMn-MIa samples inspired from the work of M. Biesinger [38]

Compound	Peak 1			Peak 2			Peak 3			Peak 4			Peak 5			Peak 6*		
	eV	%	FWHM	eV	%	FWHM	eV	%	FWHM	eV	%	FWHM	eV	%	FWHM	eV	%	FWHM
Mn(II), MnO	left to vary	23.7	1.5	Peak 1 + 0.97	27.6	1.5	Peak 1 + 1.9	21.8	1.5	Peak 1 + 2.85	12.2	1.5	Peak 1 + 3.99	5.7	1.5	Peak 1 + 5.74	9.0	left to vary
Mn(III), Mn_2O_3	left to vary	18.8	2.05	Peak 1 + 1.1	44.4	2.05	Peak 1 + 2.37	25.2	2.05	Peak 1 + 3.87	8.5	2.05	Peak 1 + 5.49	3.1	2.05			

* : MnO satellite

Table S2 : Fitting parameters used to simulate the Mn $2p_{3/2}$ envelope for xMn-MIa-AT samples inspired from the work of M. Biesinger [38]

Compound	Peak 1			Peak 2			Peak 3			Peak 4			Peak 5			Peak 6*		
	eV	%	FWHM	eV	%	FWHM	eV	%	FWHM	eV	%	FWHM	eV	%	FWHM	eV	%	FWHM
Mn(II), MnO	left to vary	34.4	1.6	Peak 1 + 1.2	26.2	1.6	Peak 1 + 2	16.9	1.6	Peak 1 + 2.9	8.6	1.6	Peak 1 + 7.5	3.5	1.6	Peak 1 + 5	10.4	left to vary
Mn(IV), MnO_2	left to vary	43.7	1.75	Peak 1 + 0.86	27.5	1.75	Peak 1 + 1.56	16.1	1.75	Peak 1 + 2.31	9.6	1.75	Peak 1 + 3.16	0.5	1.75	Peak 1 + 4.16	2.6	1.75

* : MnO satellite.

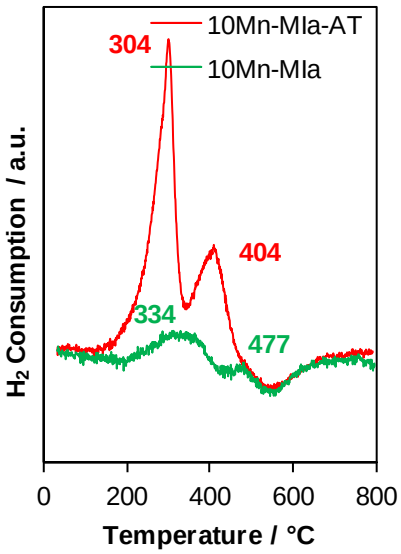

Figure S15: H_2-TPR profiles of 10Mn-MIa before and after acid treatment

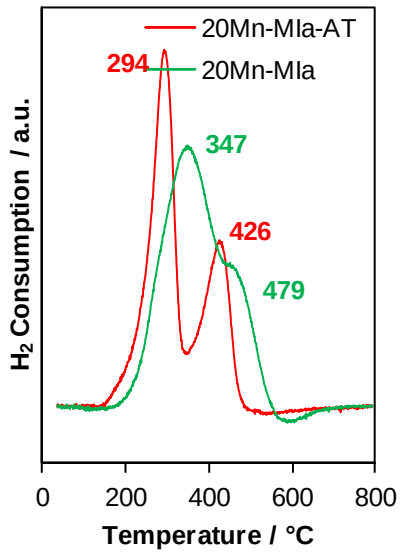

Figure S16: H_2-TPR profiles of 20Mn-MIa before and after acid treatment

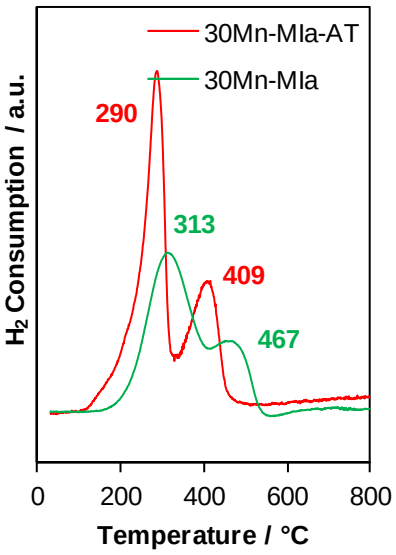

Figure S17: H_2-TPR profiles of 30Mn-MIa before and after acid treatment

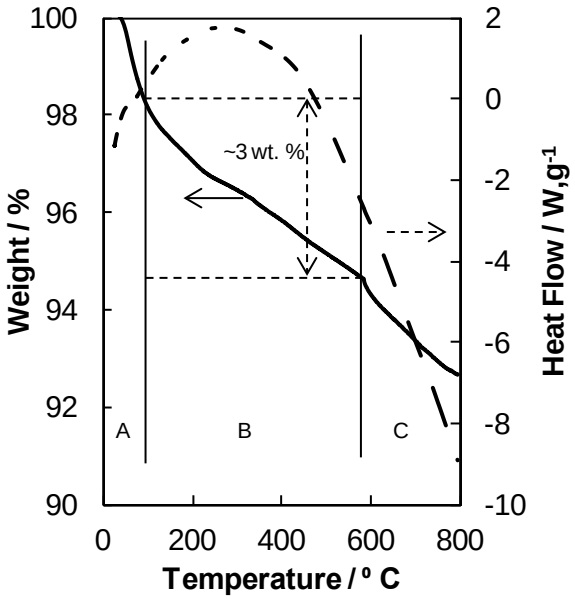

Figure S18: TGA/DSC curves of 20Mn-MIa sample

Table S3: H_2-TPR data for the xMn-MIa samples before and after acid treatment

Samples	Mn (wt%*)	H_2-consumption (mmol/g)	n_{H2} / n_{Mn}	Mn AOS
10Mn-MIa	9.41	0.071	0.04	2.1
20Mn-MIa	19.18	1.223	0.35	2.7
30Mn-MIa	26.64	1.471	0.3	2.6
10Mn-MIa-AT	2.38	0.334	0.77	3.5
20Mn-MIa-AT	8.61	0.943	0.60	3.2
30Mn-MIa-AT	10.93	1.738	0.87	3.8

*: From ICP

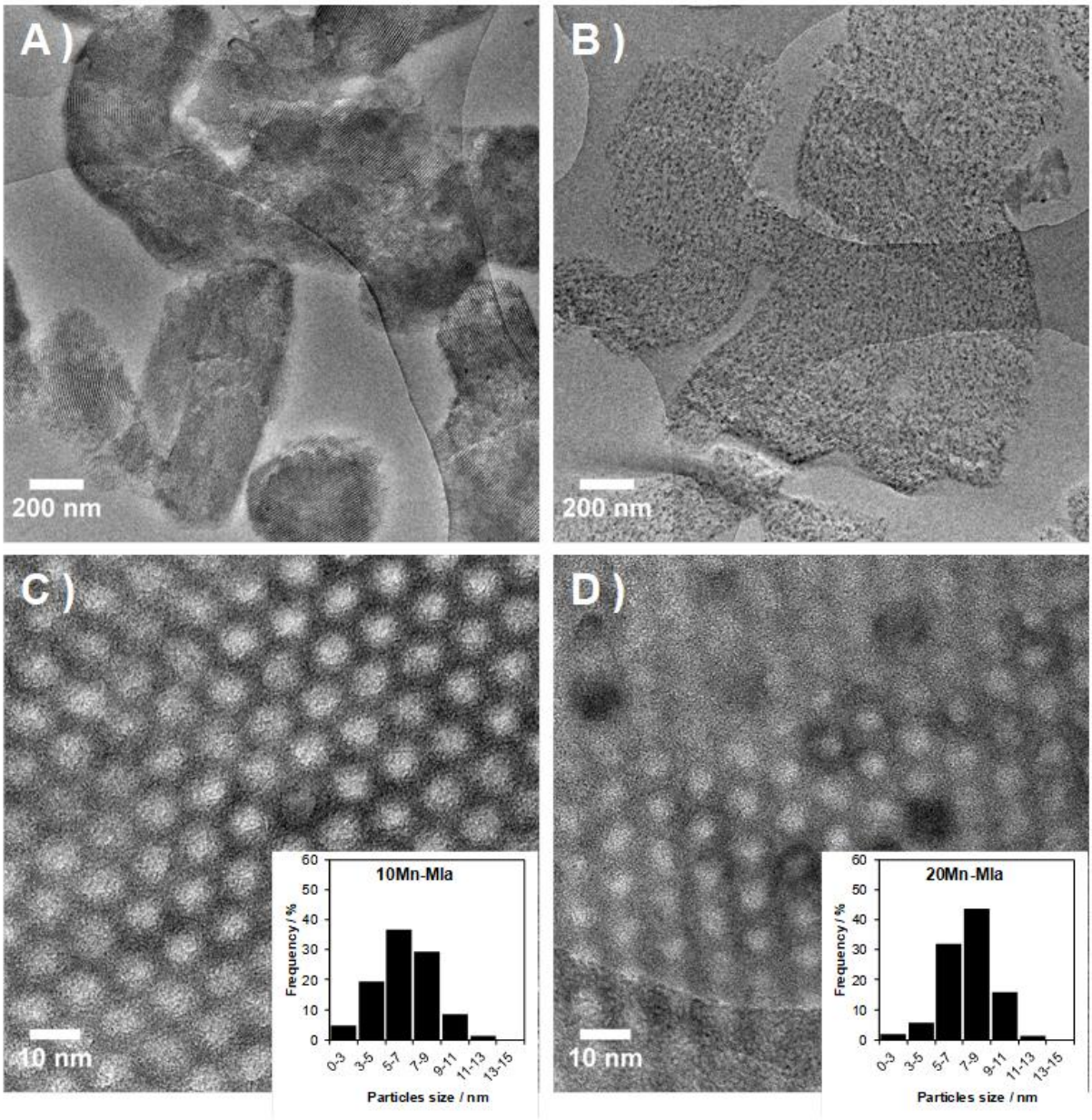

Figure S19: HR-TEM of 10Mn-MIa (A and C) and 20Mn-MIa (B and D)

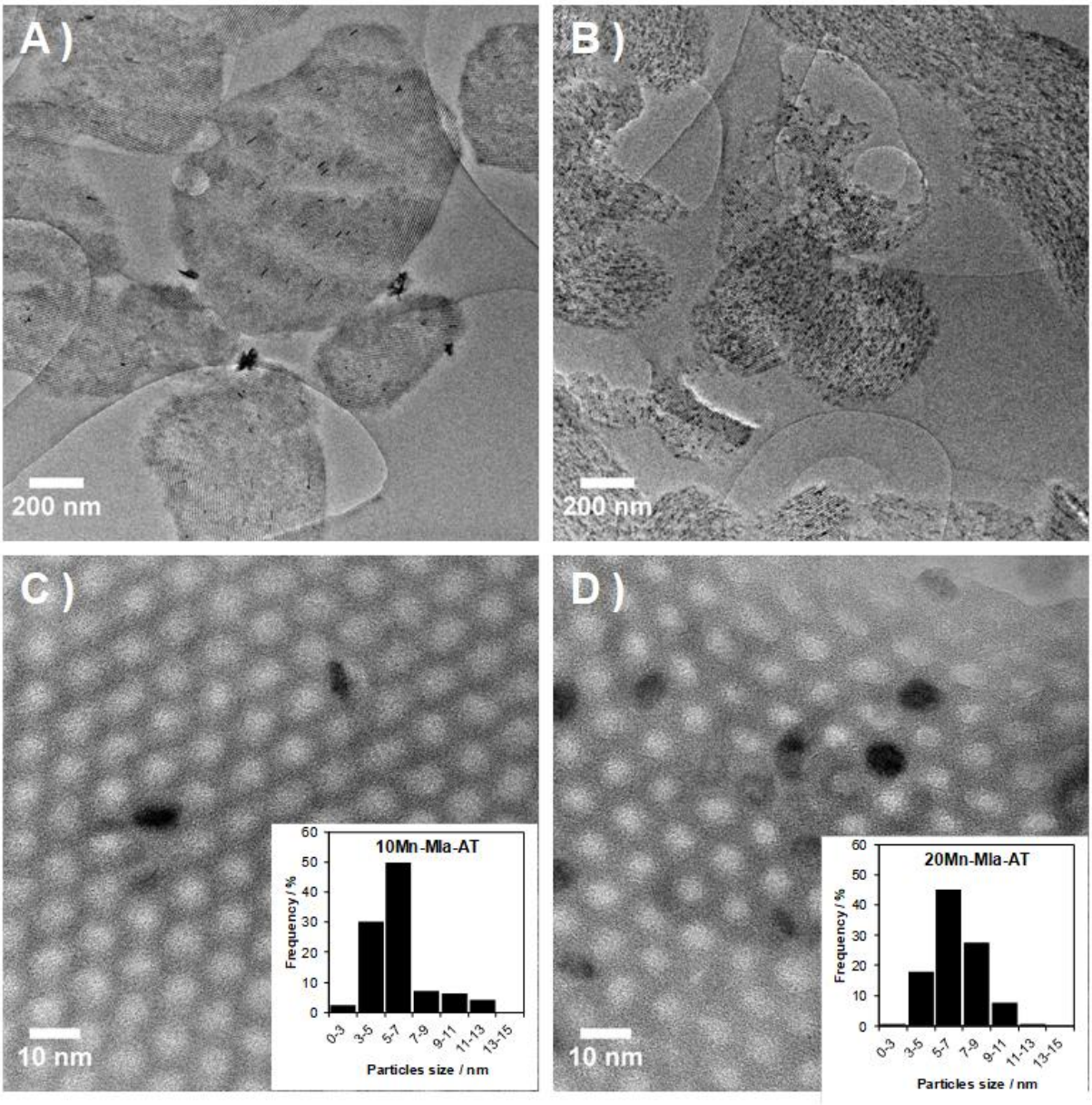

Figure S20: TEM and HR-TEM of 10-MIa-AT (A and C) and 20MIa-AT (B and D). The insert of Fig. 20(C) excludes the external particles

Table S4: Catalytic properties of the fresh and acid-treated xMn-MIa catalysts

Catalysts	T_{90} / °C	T_{50} / °C	r_s[1]
10Mn-MIa	218	183	17
20Mn-MIa	176	144	11.5
30Mn-MIa	182	141	9.5
10Mn-MIa-AT	230	205	30[2]
20Mn-MIa-AT	160	125	51.2
30Mn-MIa-AT	165	122	39.7

[1]: expressed in mmoles of HCHO converted into CO_2 per mole of Mn and per hour at 130 °C ; 2: at 170°C

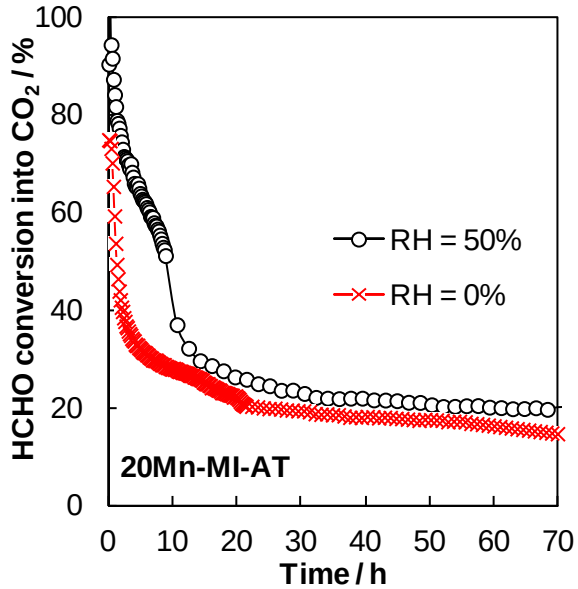

Figure S21: Plots of HCHO conversion as a function of time for 20Mn-MIa-AT in dry and humid air (RH= 50%) at 130 °C during 70 h.

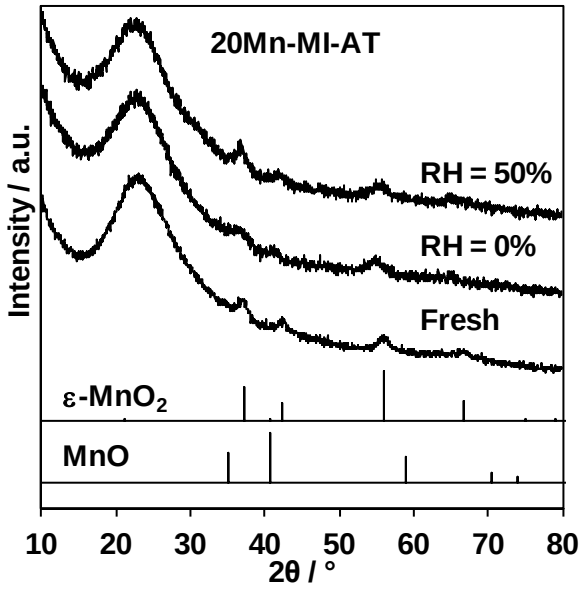

Figure S22: Wide-angle XRD patterns of fresh and used 20Mn-MIa-AT under dry or moisture condition

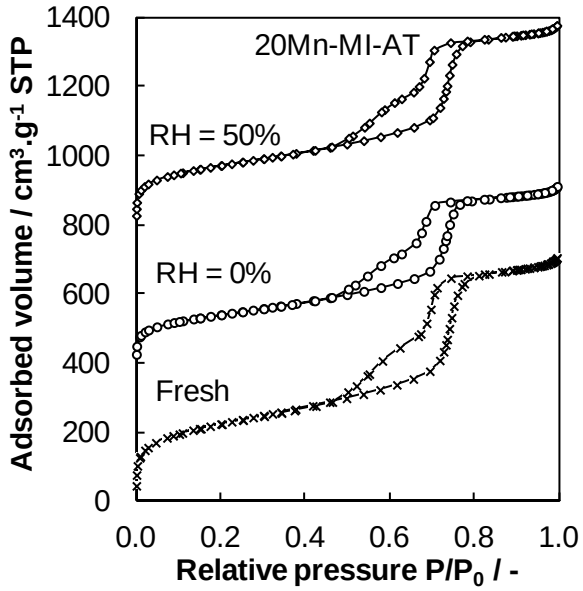

Figure S23: Adsorption / desorption isotherms (offset by 400 $cm^3.g^{-1}$) of fresh and used 20Mn-MIa-AT under dry or moisture condition

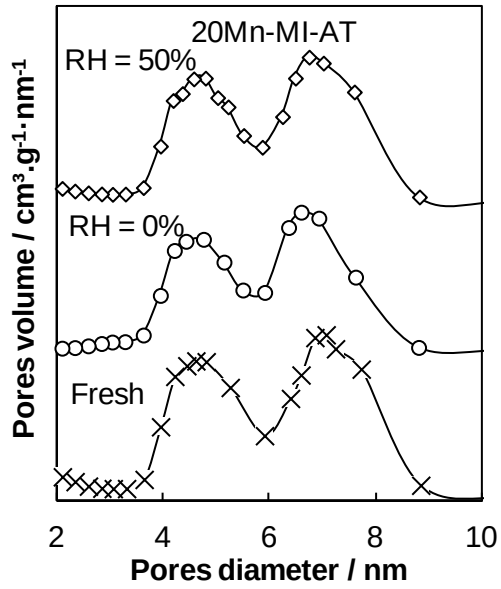

Figure S24: Pore size distribution (offset by 0.4 $cm^3.g^{-1}.nm^{-1}$) of fresh and used 20Mn-MIa-AT under dry or moisture condition

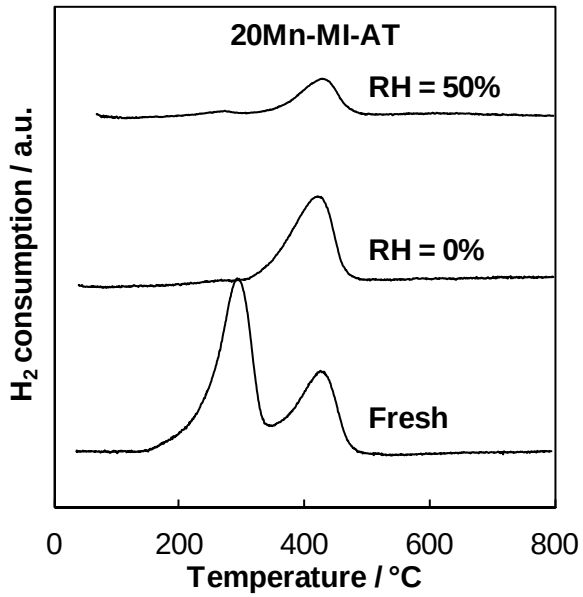

Figure S25: H_2-TPR profiles of fresh and used 20Mn-MIa-AT in dry and humid air

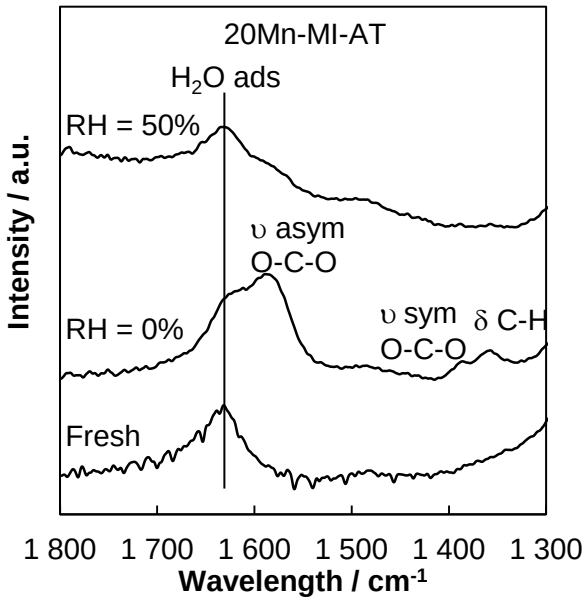

Figure S26: Evolution of infra-red spectra of fresh and used 20Mn-MIa-AT under dry or moisture condition